PHYSICAL REVIEW D **86,** 054025 (2012)

Mass spectrum and strong decays of isoscalar tensor mesons

Zao-Chen Ye ((叶早晨)),[1,2,†] Xiao Wang ((王霄)),[1,2,‡] Xiang Liu ((刘翔)),[1,2,*,§] and Qiang Zhao ((赵强))[3,4,‖]

[1]*School of Physical Science and Technology, Lanzhou University, Lanzhou 730000, China*

[2]*Research Center for Hadron and CSR Physics, Lanzhou University and Institute of Modern Physics of CAS, Lanzhou 730000, China*

[3]*Institute of High Energy Physics, Chinese Academy of Sciences, Beijing 100049, China*

[4]*Theoretical Physics Center for Science Facilities, CAS, Beijing 100049, China*

(Received 4 June 2012; published 26 September 2012)

In this work, we present a systematic study of the observed isoscalar tensor f_2 states. With the detailed analysis of the mass spectrum and calculation of the f_2 two-body strong decays, we extract information from their underlying structures and try to categorize them into the conventional tensor meson family [n^3P_2 ($n = 1, 2, 3, 4$) and m^3F_2 ($m = 1, 2$)]. We also give predictions for other decay modes of these tensor mesons, which are useful for further experimental investigations.

DOI: 10.1103/PhysRevD.86.054025 PACS numbers: 14.40.Be, 12.38.Lg, 13.25.Jx

I. INTRODUCTION

During the past few decades, there have been about 14 f_2 states with masses smaller than 2.5 GeV observed in experiment. Although the Particle Data Group (PDG) [1] has included them in the particle list, many of them have not yet been well established in experimental analysis. Taking advantage of rich experimental information, it is important to make a systematic analysis of these f_2 tensor mesons and try to understand their properties.

In the quark model, the meson typically is a bound state of a quark (q) and antiquark ($\bar{q}$), and f_2 tensor mesons have quantum numbers $I^G(J^{PC}) = 0^+(2^{++})$, which means that the relative orbital angular momentum between q and $\bar{q}$ is either $L = 1$ or $L = 3$, and the total spin is $S = 1$. Thus, to some extent the structure of the f_2 tensor meson is much more complicated compared with that of the meson with $L = 0$.

Although many f_2 tensor states were reported by experiment, a comprehensive understanding of their properties is still unavailable. First, how to categorize these observed f_2 tensor states into the $q\bar{q}$ scenario is an intriguing question since the total number of the observed f_2 states is larger than that required by the constituent quark model. It should be important to distinguish the conventional $q\bar{q}$ tensor mesons from these observed f_2 states. Second, a systematic theoretical study of the decay behavior of f_2 tensor mesons is also absent, especially their strong decays, which can provide abundant information on their internal structures [1].

In this work, we perform the mass spectrum analysis of the f_2 tensor meson family with the current experimental information. By assigning the observed states into the quark model states with similar masses, we carry out the calculation of the f_2 two-body strong decays. The calculated results can be compared with the experimental measurement of the partial decay widths.

This work is organized as follows. After the introduction, we give a brief review of the present experimental status of f_2 tensor mesons. In Sec. III, the mass spectrum analysis is presented. In Sec. IV, the strong decays of the f_2 tensor mesons are investigated in the quark pair creation (QPC) model. Finally, the paper ends with the discussion and conclusion in Sec. V.

II. RESEARCH STATUS OF f_2 TENSOR MESONS

A. Experimental observations

The present status of the so-far observed f_2 states are available in the PDG [1]. In Table I, the resonance parameters, i.e., masses and widths, are listed. Among these 14 observed f_2 states, 6 states [$f_2(1270)$, $f_2'(1525)$, $f_2(1950)$, $f_2(2010)$, $f_2(2300)$, $f_2(2340)$] are well established, while 6 states [$f_2(1430)$, $f_2(1565)$, $f_2(1640)$, $f_2(1810)$, $f_2(1910)$, $f_2(2150)$] are omitted from the summary tables of the PDG. In addition, 2 states [$f_2(1750)$, $f_2(2140)$] are listed as further states in the PDG [1]. As follows, we give a brief review of the experimental status of these states.

1. Established states

The signal of $f_2(1270)$ was first observed in Ref. [2]. Later, this state was confirmed in reactions $\pi^- p \to n2\pi^0$ [3–5], $\pi^- p \to n2K_0^S$ [6] and $\pi^- p \to 4\pi^0 n$ [7]. The BESII Collaboration observed $f_2(1270)$ in the $\pi\pi$ invariant mass spectrum of $J/\psi \to \phi\pi^+\pi^-$ [8] and $J/\psi \to \gamma\pi^+\pi^-$ [9].

$f_2'(1525)$ was reported in the reactions $\pi^- p \to K_0^S K_0^S n$ [6,10] and $\pi^- p \to K^+ K^- n$ [11,12]. Later, it was also confirmed by the Mark-III and BESII collaborations in

*Corresponding author
†yezc10@lzu.edu.cn
‡xiaowang2011@lzu.edu.cn
§xiangliu@lzu.edu.cn
‖zhaoq@ihep.ac.cn

TABLE I. The experimental information of f_2 tensor states [1]. Here, the mass and the width are average values given in units of MeV.

Established states					
State	Mass	Width	State	Mass	Width
$f_2(1270)$	1275.1 ± 1.2	$184.2^{+4.0}_{-2.4}$	$f_2'(1525)$	1525 ± 5	73^{+6}_{-5}
$f_2(1950)$	1944 ± 12	472 ± 18	$f_2(2010)$	2011^{+60}_{-80}	202 ± 60
$f_2(2300)$	2297 ± 28	149 ± 40	$f_2(2340)$	2339 ± 60	319^{+80}_{-70}
States omitted from summary table of PDG					
State	Mass	Width	State	Mass	Width
$f_2(1430)$	1430		$f_2(1565)$	1562 ± 13	134 ± 8
$f_2(1640)$	1639 ± 6	99^{+60}_{-40}	$f_2(1810)$	1815 ± 12	197 ± 22
$f_2(1910)$	1903 ± 9	196 ± 31	$f_2(2150)$	2157 ± 12	152 ± 30
Further states					
State	Mass	Width	State	Mass	Width
$f_2(1750)$	1755 ± 10	67 ± 12	$f_2(2140)$	2141 ± 12	49 ± 28

the J/ψ radiative decay $J/\psi \to \gamma K^+ K^-$ [13–16]. In addition, BESII also found $f_2'(1525)$ in $J/\psi \to \phi K\bar{K}$ [8].

$f_2(1950)$ was first reported in the reaction $K^- p \to \Lambda K\bar{K}\pi\pi$ [17], and then confirmed by OMEG in $pp \to pp2(\pi^+\pi^-)$ [18,19], $pp \to pp4\pi$ and $pp \to pp2\pi2\pi^0$ [20]. In 2000, BES Collaboration also observed $f_2(1950)$ in J/ψ radiative decay $J/\psi \to \gamma\pi^+\pi^-\pi^+\pi^-$ [21].

In 1982, a tensor structure around 2160 MeV was reported in $\pi^- p \to \phi\phi n$ by Ref. [22]. Later, the partial wave analysis of the same reaction suggested three tensor resonances, among which one resonance has a mass of 2050^{+90}_{-50} MeV [23]. This signal was confirmed by the analysis presented in Ref. [24]. This tensor structure is named as $f_2(2010)$ listed in PDG [23,24]. Besides its coupling to the $\phi\phi$ channel, $f_2(2010)$ can also decay into KK and a similar tensor structure was observed in $\pi^- p \to K_S^0 K_S^0 n$ with a mass of ~1980 MeV [25] or 2005 ± 12 MeV [26].

$f_2(2300)$ was observed in $\pi^- p \to \phi\phi n$ [22,24], $\pi^- p \to K_S^0 K_S^0 n$ [26], $\pi^- Be \to 2\phi Be$ [27]. In 2004, the Belle Collaboration also observed a structure at 2.3 GeV [28] in $\gamma\gamma \to K^+K^-$ [28], which was assigned to $f_2(2300)$.

The study of $\phi\phi$ invariant mass spectrum in $\pi^- Be \to 2\phi Be$ reaction indicated a structure around 2392 ± 10 MeV corresponding to $f_2(2340)$ [27]. This state was also observed in $\pi^- p \to \phi\phi n$ [24] and $p\bar{p} \to \eta\eta\pi^0$ [29]. Thus, the observed decay channels of $f_2(2340)$ are $\phi\phi$ and $\eta\eta$.

2. The f_2 states omitted from summary table of PDG

$f_2(1430)$ was observed in $\pi^- p \to K_S^0 K_S^0 n$ [30], which was confirmed by the ACCMOR Collaboration [31] and in Ref. [32]. Later, the Axial Field Spectrometer Collaboration found the evidence of a 2^{++} resonance with $m = 1480 \pm 50$ MeV and $\Gamma = 150 \pm 50$ MeV in $pp \to pp\pi^+\pi^-$ [33]. Although these analyses favor the same masses around 1.43–1.48 GeV, the significant width differences suggest that they should be different states.

$f_2(1565)$ was observed in antinucleon-nucleon annihilations and pion-nucleon scatterings, i.e., $\pi^- p \to \omega\omega n$ [34], $\pi^- p \to \eta\pi^+\pi^- n$ [35], $p\bar{p} \to \pi^0\eta\eta$ [36], $p\bar{p} \to \pi^0\pi^0\pi^0$ [36], $p\bar{p} \to \pi^+\pi^-\pi^0$ [37,38], and $p\bar{n} \to \pi^+\pi^+\pi^-$ [39]. The observed decay modes [1] are $\pi\pi$, $\rho^0\rho^0$, $2\pi^+\pi^-$, $\eta\eta$, and $\omega\omega$.

Signal for tensor state $f_2(1640)$ was first reported in $\pi^- p \to \omega\omega n$ [40]. The analysis of Ref. [41] suggested a tensor structure around 1650 MeV in $\pi^+\pi^+\pi^-\pi^-$ in $\bar{n}p \to 3\pi^+2\pi^-$. Bugg *et al.* performed the analysis of $J/\psi \to \gamma\pi^+\pi^+\pi^-\pi^-$, where 6 isoscalar resonances including $f_2(1640)$ were considered for fitting the data [42]. The Crystal Barrel Collaboration carried out the partial wave analysis of $p\bar{p} \to K^+K^-\pi^0$, where $f_2(1640)$ was also included [43].

The Bari-Bonn-CERN-Glasgow-Liverpool-Milano-Vienna Collaboration identified a structure around 1.8 GeV in the K^+K^- system produced in the reaction $\pi^- p \to K^+K^- n$ [44]. In Ref. [45], a tensor state at 1.8 GeV was observed when performing the amplitude analysis of the reaction $\pi^+\pi^- \to \pi^0\pi^0$. Later, the Serpukhov-Brussels-Los Alamos-Annecy (LAPP) Collaboration studied $\pi^- p \to \eta\eta n$ [46], $\pi^- p \to 4\pi^0 n$ [7], and $\pi^- p \to \pi^- p4\pi^0$ [47], where a clear peak around 1810 MeV appeared in the $4\pi^0$ mass spectrum [7,47]. The Belle Collaboration [48] measured $\eta\eta$ production in $\gamma\gamma$ fusion, and found a tensor state $f_2(1810)$. In Ref. [49], Anisovich *et al.* proposed that $f_2(1810)$ was actually the same state as the 0^+ state at 1790 MeV.

In Ref. [50], $f_2(1910)$ was first observed in the $\omega\omega$ invariant mass spectrum of $\pi^- p \to \omega\omega n$. The WA102 Collaboration reported the evidence of $f_2(1910)$ in $pp \to p_f(\omega\omega)p_s$ [51]. In order to describe $J^{PC} = 2^{++}$ amplitudes in the $\omega\omega$ system, $f_2(1910)$ was needed in addition to $f_2(1565)$ [34], and decay information for $f_2(1910) \to \omega\omega$ can be extracted.

The last tensor state omitted from PDG is $f_2(2150)$. The WA102 Collaboration found the signal of $f_2(2150)$

in $pp \to p_f(\eta\eta)p_s$ [52] and determined the ratio $B(f_2(2150) \to \eta\eta)/B(f_2(2150) \to K\bar{K}) = 0.78 \pm 0.14$. Further experimental information on $f_2(2150)$ can be found in PDG [1].

3. Further states

In 2006, $f_2(1750)$ was reported by analyzing $\gamma\gamma to K_S^0 K_S^0$ in Ref. [53], where the data were collected by the L3 experiment at LEP. The resonance parameters of $f_2(1750)$ are listed in Table I. The partial widths of $f_2(1750)$ decays into $K\bar{K}$, $\pi\pi$, and $\eta\eta$ are 17 ± 5, 1.3 ± 1.0, and 2.0 ± 0.5 MeV, respectively, [53]. In addition, by the $SU(3)$ analysis, the mixing angles between nonstrange $(n\bar{n} = (u\bar{u} + d\bar{d})/\sqrt{2})$ and strange $(s\bar{s})$ components are determined as $-1 \pm 3^\circ$ and $-10^{+5}_{-10}{}^\circ$ [53], which correspond to two tensor nonets $[f_2(1270), f_2'(1525), a_2(1320)]$ and $[f_2(1560), f_2(1750), a_2(1700)]$, respectively.

As a narrow enhancement, $f_2(2140)$ was observed in ϕK^+K^- and $\phi\pi^+\pi^-$ final states, which are produced in p-N interaction [54].

B. Theoretical progress

In the past decades, there have been many theoretical studies of the properties of the tensor f_2 states. In the following, we give a brief summary for the theoretical status of f_2 states.

Lattice QCD calculations predict that the mass of a tensor glueball is around 2.3 GeV. It has thus initiated experimental motivations for the search of the glueball candidate in the study of the isoscalar tensor spectrum [55,56]. Bugg and Zou indicated that the 2^{++} glueball mixing with $q\bar{q}$ and $s\bar{s}$ states with 2^3P_2 can explain why the mass of the observed $f_2(1565)$ is lower than the expected one [57]. In Ref. [58], Barnes *et al.* calculated the strong decays of tensor meson with 2^3P_2, where the mass of this state is taken as 1700 MeV. The result shows that $\rho\rho$, $\omega\omega$, $\pi\pi$, and πa_2 are its important decay channels. Later, the decays of several f_2 mesons with 1^3P_2, 2^3P_2, and 1^3F_2 were calculated using the $^3P_0$ model [59]. By extending the Nambu-Jona-Lasinio model, authors of Ref. [60] carried out the covariant calculation of the properties of f_2 mesons. The calculated masses can be consistent with the corresponding experimental data of f_2 states below 2 GeV. Here, the obtained f_2 states with the $s\bar{s}$ component are around 1551 and 1767 GeV, respectively, which also explains $f_2'(1525)$ and $f_2(1750)$ as 1P and 2P $s\bar{s}$ state in the f_2 family, respectively, [60]. With the chiral perturbation theory, Dobado *et al.* studied the elastic pion scattering in the $I = 0$ and $J = 2$ channel. They found that $f_2(1270)$ can be described well as a pole in the second Riemann sheet [61]. Ebert *et al.* calculated the mass spectra of light mesons by the relativistic quark model [62]. Reference [63] provides a coupled-channel analysis of the data of $\pi\pi \to \pi\pi$, $K\bar{K}$, $\eta\eta$, and $f_2(1270)/f_2'(1525)$, and $f_2(1600)/f_2(1710)$ extracted from the experimental data are categorized as the first and the second tensor nonets, respectively. In Ref. [64], the decays of the low-lying tensor mesons into both two pseudoscalar and pseudoscalar-vector were studied and have shown to be in agreement with the $q\bar{q}$ interpretation. Moreover, the glueball candidate $f_J(2220)$ was also studied.

In the mixing scheme of $f_2(1270)$ and $f_2'(1525)$, Li *et al.* obtained the isoscalar singlet-octet mixing angle ($\theta = 27.5^\circ$) and estimated the decays of $f_2(1270)$ and $f_2'(1525)$ [65]. Cheng and Shrock studied the mixing of $f_2(1270)$ and $f_2'(1525)$ [66], where the mixing angle of the flavor SU(3) singlet and octet was determined as $\theta_{T,\mathrm{ph}} = 29.5^\circ$ consistent with the value listed in PDG [1].

Roca and Oset suggested that $f_2(1270)$, $\rho_3(1690)$, $f_4(2050)$, $\rho_5(2350)$, and $f_6(2510)$ are multi-$\rho(770)$ states [67]. In Ref. [68], the authors studied the productions of $f_2(1270)$ and $f_2'(1525)$ via $J/\psi \to \phi(\omega)f_2(1270)$ and $J/\psi \to \phi(\omega)f_2'(1525)$, respectively, where $f_2(1270)$ and $f_2'(1525)$ are identified as the dynamically generated states via the vector-vector interactions from the hidden gauge formalism [69]. The radiative decays $J/\psi \to \gamma f_2(1270)$ or $\gamma f_2'(1525)$ were calculated in Ref. [70], and the two-photon and one photon-one vector meson decay widths of $f_2(1270)$, $f_2'(1525)$ were obtained by treating $f_2(1270)$ and $f_2'(1525)$ as the dynamically generated states [71]. Ma performed a QCD analysis for the radiative decay of heavy quarkonium with $^3S_1$ into $f_2(1270)$ and calculated the ratios of $B(\Upsilon \to \gamma f_2(1270))$ to $B(J/\psi \to \gamma f_2(1270))$, where the obtained ratios are in agreement with the experimental value [72].

Besides the above theoretical work under the framework of the conventional meson framework, many theoretical efforts have been made in order to single out evidence for the isoscalar tensor glueball. The glueball-$q\bar{q}$ mixing was studied using Schwinger-type mass formulas in Ref. [73], which suggested that $f_J(2220)$ should be a tensor glueball candidate. It was also shown that $f_2(1810)$ might have a large glueball component. In contrast, the decay of $f_2'(1525) \to \pi\pi$ was consistent with its being a $q\bar{q}$ state [73]. The relativistic flux tube model was applied to investigate the meson and glueball spectra, where $f_2(1950)$ and $f_2(2010)/f_2(2300)$ can be assigned as a pure $n\bar{n}$ and $s\bar{s}$ states, respectively, while $f_2(2340)$ was suggested as a good candidate of tensor glueball [74]. In Ref. [75], the mixing scheme of $f_2(1270)$, $f_2'(1525)$ and the 2^{++} glueball was proposed. It shows that different models have quite different prescriptions for the classification of those observed tensor states. Because of this, it is of great importance to provide a systematic study of the tensor meson spectrum for any approaches. We emphasize again that this controversial status of the isoscalar tensor spectrum motivates us to make a systematic analysis of the strong decays of those tensor states. More details about the experimental

and theoretical status of the tensor glueball studies can be found in Refs. [76–79].

III. MASS SPECTRUM ANALYSIS

As summarized in Sec. II A, there exist abundant experimental observations of f_2 states beyond the $q\bar{q}$ scenario. As a starting point of categorizing these states, we first try to accommodate these states into the Regge trajectories for the mass spectrum [80], i.e.,

$$M^2 = M_0^2 + (n-1)\mu^2, \tag{1}$$

where parameters M_0, n, and μ^2 denote the mass of ground state, radial quantum number and the slope parameter of the trajectory, respectively. As shown in Ref. [80], μ^2 is usually in the range of 1.10–1.40 GeV^2 to give a reasonable description of the experimental data.

As a guidance for our categorizing the f_2 states, we give a comparison of the experimental data listed in Table I and the result from the analysis of Regge trajectories with slope $\mu^2 = 1.10$ GeV^2 and $\mu^2 = 1.25$ GeV^2 for P-wave and F-wave f_2 mesons, respectively. Since $f_2(1270)$ and $f_2'(1525)$ can be the ground states of $^{2s+1}J_L = {}^3P_2$ tensor with flavor contents $n\bar{n} = (u\bar{u} + d\bar{d})/\sqrt{2}$ and $s\bar{s}$, respectively, the corresponding Regge trajectories start from $(n, M_0^2) = (1, 1.270^2)$ and $(1, 1.525^2)$ as shown in Fig. 1. One notices that the number of tensor states listed in Table I is more than that of states in the $q\bar{q}$ scenario. It indicates several possibilities: i) the signals with close masses could be due to the same state; ii) some states cannot be accommodated into the $q\bar{q}$ tensor meson family; iii) some signals might be produced by artificial effects, thus, should be omitted. Since how to distinguish these states is beyond the scope of this work, we simply list those states with close masses in Table I when comparing with the result from the analysis of Regge trajectories.

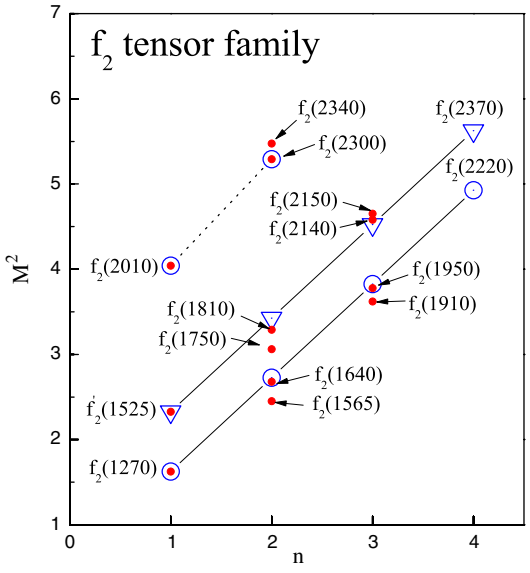

FIG. 1 (color online). The analysis of Regge trajectories for the mass spectrum of f_2 family. Here, the symbols $\bigtriangledown$ and $\odot$ stand for the theoretical values of $n\bar{n}$ and $s\bar{s}$ states, respectively, which are obtained by Eq. (1) with $\mu^2 = 1.10$ GeV^2 and $\mu^2 = 1.25$ GeV^2 for P-wave (black solid lines) and F-wave (black dashed lines) f_2 mesons, respectively. While the experimental data are marked by red dots.

The result shown in Fig. 1 indicates that $[f_2(1565)/f_2(1640),\ f_2(1750)/f_2(1810)]$, $[f_2(1910)/f_2(1950),\ f_2(2120)/f_2(2140)/f_2(2150)]$ and $[f_2(2220), f_2(2370)]$ can be organized as the first, second, and third radial excitations of $[f_2(1270), f_2'(1525)]$, respectively. As discussed above, we cannot distinguish $f_2(1565)$ and $f_2(1640)$ by the analysis of Regge trajectories since their masses are close to each other. The situations for $f_2(1750)/f_2(1810)$, $f_2(1910)/f_2(1950)$, and $f_2(2140)/f_2(2150)$ are similar to that of $f_2(1565)/f_2(1640)$. Thus, further study of strong decay behavior of these f_2 states will be helpful to clarify their properties. The details will be given in Sec. IV.

We also try to group those P-wave f_2 mesons in association with the corresponding a_2 and K_2 mesons to form tensor nonets, i.e.,

$$\begin{aligned}
&1P\text{: } f_2(1270),\ f_2'(1525),\ a_2(1320),\ K_2^*(1430),\\
&2P\text{: } \begin{Bmatrix} f_2(1565) \\ f_2(1640) \end{Bmatrix},\ \begin{Bmatrix} f_2(1750) \\ f_2(1810) \end{Bmatrix},\ a_2(1700),\ K_2^*(?),\\
&3P\text{: } \begin{Bmatrix} f_2(1910) \\ f_2(1950) \end{Bmatrix},\ \begin{Bmatrix} f_2(2140) \\ f_2(2150) \end{Bmatrix},\ a_2(1950),\ K_2^*(1980),\\
&4P\text{: } f_2(2220),\ f_2(2370),\ a_2(2250),\ K_2^*(?),
\end{aligned}$$

where two tensor $K_2^*(?)$ mesons corresponding to $2P$ and $4P$ states are absent in experiment.

The mass spectrum analysis shown in Fig. 1 also indicates that $f_2(2010)$ and $f_2(2300)$ are possible candidates for the 1^3F_2 and 2^3F_2 states, respectively, when taking the slope $\mu^2 = 1.25$ GeV^2. In the next section, we will discuss the possibility of treating the reported $f_2(2300)$ or $f_2(2340)$ as the first radial excitation of $f_2(2010)$.

IV. STRONG DECAY BEHAVIOR

For obtaining the two-body strong decay behavior of these discussed f_2 states, we adopt the QPC model [81], which has been extensively applied to the study of the strong decay of hadrons [82–106]. For the calculation of two-body strong decay of a hadron, the operator T accounting for the $q\bar{q}$ creation from the vacuum is introduced by

$$\begin{aligned}
T = -3\gamma \sum_m \langle 1m; 1-m|00\rangle \int d\boldsymbol{k}_3 d\boldsymbol{k}_4 \delta^3(\boldsymbol{k}_3 + \boldsymbol{k}_4) \\
\times \mathcal{Y}_{1m}\left(\frac{\boldsymbol{k}_3 - \boldsymbol{k}_4}{2}\right) \chi^{34}_{1,-m} \varphi_0^{34} \omega_0^{34} d_{3i}^\dagger(\boldsymbol{k}_3) b_{4j}^\dagger(\boldsymbol{k}_4),
\end{aligned} \tag{2}$$

where the definitions of flavor singlet, color singlet, and the ℓth solid harmonic polynomial are as follows

$$\varphi_0^{34} = \frac{u\bar{u} + d\bar{d} + s\bar{s}}{\sqrt{3}}, \qquad \omega_0^{34} = \frac{1}{\sqrt{3}}\delta_{\alpha_3\alpha_4}(\alpha = 1, 2, 3),$$
$$\mathcal{Y}_{\ell m}(\boldsymbol{k}) = |\boldsymbol{k}|^{\ell} Y_{\ell m}(\theta_k, \phi_k).$$

In Eq. (2), i and j are the $SU(3)$ color indices of the created quark and antiquark, and $\chi^{34}_{1,-m}$ denotes a spin triplet state.

The transition matrix element for A decay into B and C can be expressed in terms of the helicity amplitude as

$$\langle BC|T|A\rangle = \delta^3(\boldsymbol{K}_B + \boldsymbol{K}_C - \boldsymbol{K}_A)\mathcal{M}^{M_{J_A}M_{J_B}M_{J_C}}. \quad (3)$$

By the Jacob-Wick formula [107], the partial wave amplitude $\mathcal{M}^{JL}$ can be further related to the helicity amplitude $\mathcal{M}^{M_{J_A}M_{J_B}M_{J_C}}$. Thus, the partial decay width can be written as

$$\Gamma = \pi^2 \frac{|\boldsymbol{K}|}{M_A^2} \sum_{JL} |\mathcal{M}^{JL}|^2, \quad (4)$$

where $|\boldsymbol{K}|$ is the three momentum of the daughter hadrons in the initial state center of mass (c.m.) frame.

In Eq. (5), a dimensionless parameter γ is introduced for describing the strength of the quark pair creation from the vacuum. It can be extracted by fitting the experimental data, for which 15 decay channels are included as listed in Table II. In the numerical calculation of the partial decay width, we adopt the harmonic oscillator wave function for the spatial wave function of the meson, i.e., $\Psi_{n,\ell m}(R, \boldsymbol{k}) = \mathcal{R}_{n,\ell}(R, \boldsymbol{k})\mathcal{Y}_{n,\ell m}(\boldsymbol{k})$, where R is determined by reproducing the realistic root mean square radius by solving the Schrödinger equation with the linear potential [96,105], i.e., we have relation

$$\sqrt{\langle r^2\rangle} \equiv \left(\int \Psi^*_{n,\ell m}(R, \boldsymbol{r}) r^2 \Psi_{n,\ell m}(R, \boldsymbol{r}) d^3r\right)^{1/2},$$

where $\sqrt{\langle r^2\rangle}$ is from solving the Schrödinger equation with the linear potential. By this relation, we finally get the R value for the corresponding meson. The resonance parameters of the mesons involved in our calculation are taken from the data listed in PDG [1].

We define $\chi^2 = \sum_i (\Gamma_i^{\text{theory}} - \Gamma_i^{\text{exp}})^2/\delta^2_{\Gamma_i}$, where δ_{Γ_i} denotes the average experimental error of each partial decay width. By minimizing χ^2, we obtain $\gamma_0 = 8.7$, and the corresponding experimental data and theoretical results are shown in Table II.

In the following, we present the numerical results for the partial decay widths of those isoscalar tensor states.

TABLE II. The measured partial decay widths of 16 decay channels and the comparison with theoretical calculation (the third column). Here, the minimum of χ^2 is 2149.

Decay channel	Measured width (MeV) [1]	QPC (MeV)
$b_1(1235) \to \omega\pi$	142 ± 8	119.5
$\phi \to K^+K^-$	2.08 ± 0.02	1.82
$a_2(1320) \to \eta\pi$	15.5 ± 0.7	22.6
$a_2(1320) \to K\bar{K}$	5.2 ± 0.2	2.1
$\pi_2(1670) \to f_2(1270)\pi$	145.8 ± 5.1	118.7
$\pi_2(1670) \to \rho\pi$	80.3 ± 2.8	70.1
$\rho_3(1690) \to \pi\pi$	38 ± 2.4	57.9
$\rho_3(1690) \to \omega\pi$	25.8 ± 1.6	71.7
$\rho_3(1690) \to K\bar{K}$	2.5 ± 0.2	1.3
$K^*(892) \to K\pi$	48.7 ± 0.8	28.4
$K^*(1410) \to K\pi$	15.3 ± 1.4	13.3
$K_0^*(1430) \to K\pi$	251 ± 74	165.5
$K_2^*(1430) \to K\pi$	54.4 ± 2.5	66.8
$K_2^*(1430) \to K^*(892)\pi$	26.9 ± 1.2	33.6
$K_2^*(1430) \to K\rho$	9.5 ± 0.4	13.2
$K_2^*(1430) \to K\omega$	3.16 ± 0.15	3.9

A. The ground states in the tensor meson family

As the candidate of 1^3P_2 tensor states, $f_2(1270)$ and $f_2'(1525)$ can be regarded as the mixture of $N = (u\bar{u} + d\bar{d})/\sqrt{2}$ and $S = s\bar{s}$

$$|f_2(1270)\rangle = \sin\phi|N\rangle + \cos\phi|S\rangle, \quad (5)$$

$$|f_2'(1525)\rangle = \cos\phi|N\rangle - \sin\phi|S\rangle \quad (6)$$

with $\phi \equiv \theta + 54.7°$, where θ is the mixing angle between the SU(3) flavor singlet and octet. In our calculation, we take $\theta = 29.6°$ from PDG [1], which corresponds to $\phi = 84.3°$. In Ref. [64], a similar value for the mixing angle θ was found.

In Fig. 2, we present the calculated partial decay widths of $f_2(1270)$ and $f_2'(1525)$ in terms of parameter R within a typical range of values. For $f_2(1270)$, our calculation indicates that $\pi\pi$ channel is its dominant decay mode and $\Gamma(f_2(1270) \to K\bar{K}) > \Gamma(f_2(1270) \to \eta\eta)$. These decay behaviors are consistent with the experimental observation [1]. We also notice that the PDG data ($\Gamma_{\eta\eta} = 0.74 \pm 0.14$ MeV) [1] can be described by our calculation of the decay width of $f_2(1270) \to \eta\eta$ well. However, the obtained $\Gamma(f_2(1270) \to K\bar{K})$ is about 0.27–0.35 times smaller than the data [1].

The sum of the theoretical two-body strong decays of $f_2(1270)$ can reach up to $120.5 \sim 97.5$ MeV corresponding to $R = 3.2$–4.2 GeV^{-1}. This value is smaller than the experimental average width $\Gamma_{f_2(1270)} = 184.2^{+4.0}_{-2.4}$ MeV [1], but comparable with the results of measurements of Refs. [2,108]. Actually, there still exist large experimental discrepancies among different experimental measurements of the $f_2(1270)$ width as listed in PDG [1]. Further experimental study of the resonance parameter of $f_2(1270)$ is still needed. In addition, we note that we do not include the partial width of $f_2(1270)$ decays into multipions (the sum of the branching ratios of $f_2(1270) \to \pi^+\pi^-2\pi^0$, $2\pi^+2\pi^-$ is about 9.9% [1]) when making the comparison between our calculation and the experimental data. Thus, the difference between our result and the central value of the $f_2(1270)$ width [2] shown in Fig. 2 can be understood.

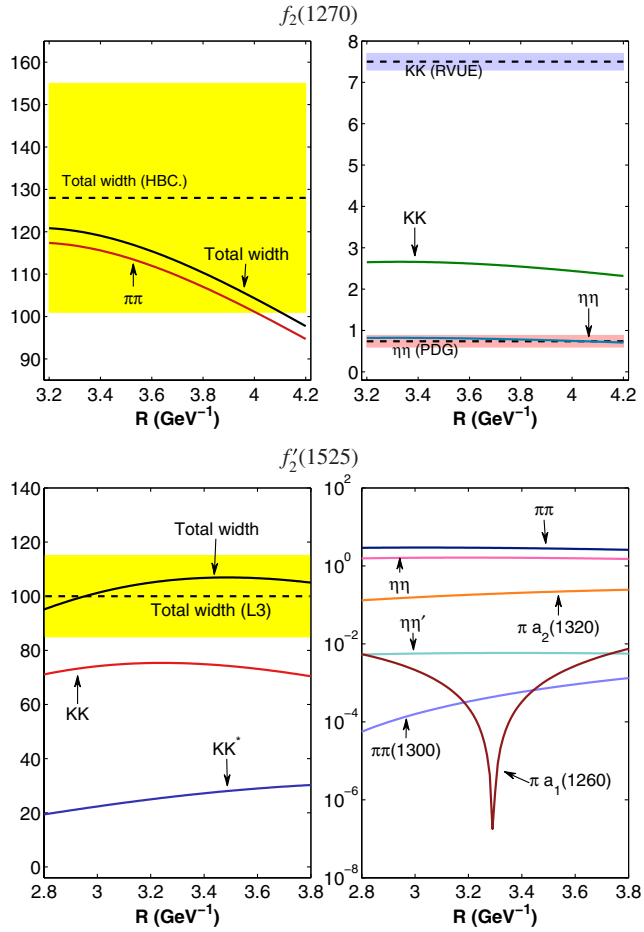

FIG. 2 (color online). The obtained two-body partial decay widths of $f_2(1270)$ and $f_2'(1525)$ dependent on the R value and the comparison with the experimental data (the dashed lines with bands). Here, the experimental width of $f_2(1270)$ and $f_2'(1525)$ are taken from Refs. [2,109], respectively. The experimental partial widths of $f_2(1270)$ decays into $K\bar{K}$ and $\eta\eta$ are given by Refs. [1,53], respectively.

The results for $f_2'(1525)$ is presented in the lower panel of Fig. 2. The sum of the two-body strong decays of $f_2'(1525)$ calculated in this work overlaps with the experimental data from seven experiments, i.e., 108^{+5}_{-2} [6], 102 ± 42 [108], 100 ± 15 [109], 90 ± 12 [110], 103 ± 30 [14], 104 ± 10 [53], and 100 ± 3 MeV [111]. The calculated $\Gamma(f_2'(1525) \to K\bar{K})$ is about 70.4–75.3 MeV corresponding to $R = 2.8$–3.8 GeV^{-1}, which is comparable with the experimental average value 65^{+5}_{-4} MeV listed in PDG [1]. Our result suggests $\Gamma(f_2'(1525) \to K\bar{K}^* + \text{H.c.})$ is about 24.1 MeV ($R = 3.125$ GeV^{-1}), which shows that $K\bar{K}^* +$ H.c. is an important decay channels of $f_2'(1525)$. We also suggest future experiment to carry out the search for $f_2'(1525)$ in the $K\bar{K}^* + \text{H.c.}$ decay channel. We obtain $\Gamma(f_2'(1525) \to \eta\eta) = 1.63$ MeV with the typical value $R = 3.125$ GeV^{-1}, which is smaller than the experimental data ($\Gamma_{\eta\eta} = 5 \pm 0.8$ MeV [53]). The obtained $\Gamma(f_2'(1525) \to \pi\pi) = 2.94$ MeV with the typical value $R = 3.125$ GeV^{-1} is also comparable with the data $\Gamma_{\pi\pi} = 1.4^{+1.0}_{-0.5}$ MeV [6]. It should be noted that the partial width of $f_2'(1525) \to \pi\pi$ is sensitive to the mixing angle ϕ.

TABLE III. Several ratios of the partial decay widths of $f_2(1270)$ and $f_2'(1525)$, and the comparison with the experimental data.

States	Ratios	This work	Experimental data
$f_2(1270)$	$\Gamma_{K\bar{K}}/\Gamma_{\pi\pi}$	0.0239	0.041 ± 0.005 [1]
	$\Gamma_{\eta\eta}/\Gamma_{\pi\pi}$	0.0073	0.003 ± 0.001 [52]
	$\Gamma_{\eta\eta}/\Gamma_{\text{total}}$	0.0068	0.004 ± 0.0008 [1]
$f_2'(1525)$	$\Gamma_{\eta\eta}/\Gamma_{K\bar{K}}$	0.0217	0.115 ± 0.028 [1]
	$\Gamma_{\pi\pi}/\Gamma_{K\bar{K}}$	0.0393	0.075 ± 0.035 [112]
	$\Gamma_{\pi\pi}/\Gamma_{\text{total}}$	0.0286	$0.027^{+0.071}_{-0.013}$ [11]

Additionally, several partial decay width ratios of $f_2(1270)$ and $f_2'(1525)$ are calculated and listed in Table III to compare with the corresponding experimental values.

B. $n^{2S+1}L_J = 2^3P_2$ tensor mesons

As indicated in Fig. 1, the analysis of Regge trajectories supports $f_2(1640)$ and $f_2(1810)$ to be the candidates of 2^3P_2 tensor states. Different from these two ground states discussed above, the information of the mixing angle of $f_2(1640)$ and $f_2(1810)$ are still unclear at present. In a realistic picture, $f_2(1640)$ and $f_2(1810)$ cannot be as pure $n\bar{n}$ and $s\bar{s}$ states, respectively. Thus, we take the range of ϕ ($\phi = (75$–$90)°$) when calculating the strong decays of $f_2(1640)$ and $f_2(1810)$, where $\phi = 90°$ denotes $f_2(1640)/f_2(1810)$ as the pure $n\bar{n}/s\bar{s}$ state.

If $f_2(1640)$ are the first radial excitation of $f_2(1270)$, the obtained total width of its two-body strong decay overlaps with the MARK3 data [42] as shown in Fig. 3. The main decay channels of $f_2(1640)$ are $\pi\pi$, $\pi a_1(1260)$, and $\pi\pi(1300)$. In addition, several important decays of $f_2(1640)$ include $\rho\rho$, $\omega\omega$ and $\pi a_2(1320)$, which are dependent on R value due to the node effect. In experiment, $f_2(1640) \to \omega\omega$ was reported in Ref. [40]. The 4π channel of $f_2(1640)$ decays was also observed in Ref. [40]. If it is due to the $\rho\rho$ contribution, our calculation turns out to be consistent with this observation. The $f_2(1640) \to K\bar{K}$ decay width shown in Fig. 3 is supported by the experimental observation of Ref. [43]. The result in Fig. 3 indicates that its $K\bar{K}$, $K\bar{K}^* + \text{H.c.}$ and $\eta\eta$ decay channels are sensitive to the mixing angle ϕ, which can be interesting channels to test the mixing angle.

Although we take $f_2(1640)$ as the candidate of the first radial excitation of $f_2(1270)$, we can actually compare our result with the experimental information of $f_2(1565)$ since our results are insensitive to the mass of the initial state. As listed in PDG [1], the reported decay channel of $f_2(1565)$ are $\pi\pi$, $\rho\rho$, $\eta\eta$, $\omega\omega$, $K\bar{K}$, which are also supported by our result in Fig. 3.

At present, $f_2(1640)$ and $f_2(1565)$ are not classified as the established states in PDG. According to our

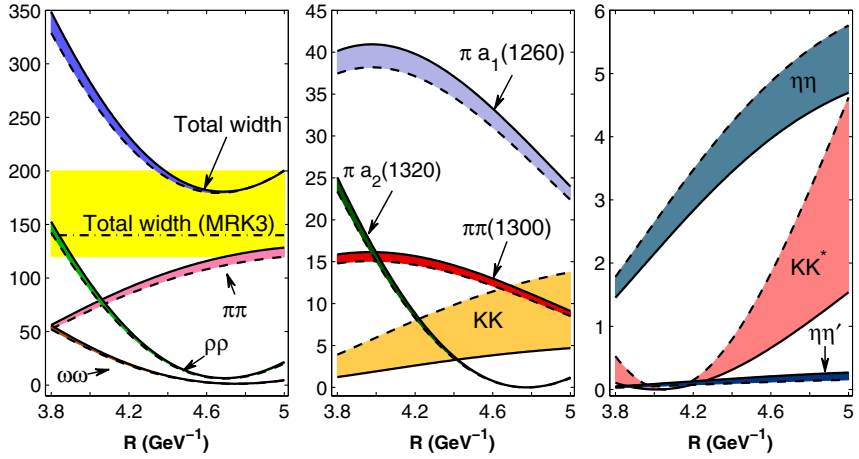

FIG. 3 (color online). The partial decay width of $f_2(1640)$ dependent on the R value and the comparison with the experimental data (the dash-dot lines with yellow band from Ref. [42]). Here, the solid and dashed lines are the results taking the typical values $\phi = 90°$ and $\phi = 75°$, respectively.

calculation, $\pi\pi$ is the dominant decay channel of $f_2(1640)$. However, the $f_2(1640) \to \pi\pi$ decay is still missing in experiment. We need to find a suitable reason to explain the absence of the $f_2(1640) \to \pi\pi$ decay. Besides the mass difference of $f_2(1640)$ and $f_2(1565)$, we notice that both $f_2(1640)$ and $f_2(1565)$ are of similar decay behaviors. Thus, we suggest further experiment to examine whether $f_2(1640)$ and $f_2(1565)$ are the same state, and clarify why $f_2(1640) \to \pi\pi$ is absent in experiment while $f_2(1565) \to \pi\pi$ has been observed. In Ref. [113], Baker *et al.* once indicated that $f_2(1565)$ and $f_2(1640)$ could be the same resonance. Since the $\omega\omega$ decay mode of $f_2(1565)$ has a relatively high threshold, the resonance peak position is shifted to higher mass of 1640 MeV.

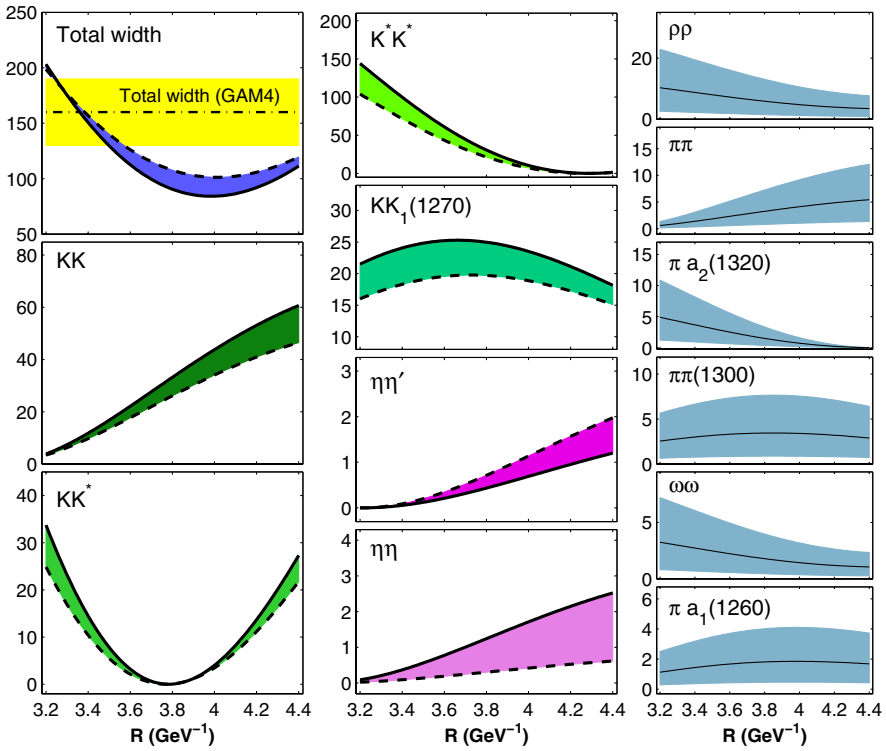

FIG. 4 (color online). The two-body strong decay widths of $f_2(1810)$ dependent on the R value and mixing angle ϕ. The solid and dashed lines in each diagram shown in the first and second columns correspond to the results taking the typical value $\phi = 85°$ and $\phi = 75°$, respectively. Here, the experimental width (the dash-dot line with yellow band) of $f_2(1810)$ is taken from Ref. [47]. The bands appearing in the diagrams in the third column are due to $\phi = (75\text{–}85)°$ taken in our calculation, where the solid lines are the typical values with $\phi = 80°$.

In Fig. 4, the partial decay widths of $f_2(1810)$ as the first radial excitation of $f_2'(1525)$ are given. We find that the calculated total width of $f_2(1810)$ is consistent with the experimental data [47] when taking $R = 3.37$ GeV^{-1}. The dominant decay of $f_2(1810)$ is $K^*\bar{K}^*$ while other sizeable decays include $K\bar{K}$, $K\bar{K}^*$, $KK_1(1270)$. As the mixing state of $n\bar{n}$ and $s\bar{s}$, $f_2(1810)$ can also decay into $\rho\rho$, $\pi\pi$, $\pi\pi(1300)$, $\omega\omega$, and $\pi a_2(1320)$, which are shown in the third column of Fig. 4. It shows that the obtained partial widths are strongly dependent on the mixing angle ϕ due to the dominance of the $s\bar{s}$ component in the $f_2(1810)$ flavor wave function. Taking $\phi = 85°/75°$ and $R = 3.37$ GeV^{-1}, we obtain the typical values of the partial widths of $f_2(1810)$, i.e., the decay widths of $K^*\bar{K}^*$, $K\bar{K}_1(1270) + \text{H.c.}$, $K\bar{K}^* + \text{H.c.}$, and $K\overline{K}$ are, respectively, 106.2/76.3, 23.8/18.0, 16.9/12.2, and 10.4/8.6 MeV.

As the further states listed in PDG [1], the masses of $f_2(1750)$ and $f_2(1810)$ are close to each other. Because the results presented in Fig. 4 are not strongly dependent on the mass of the initial state, we also compare our result with the experimental data for $f_2(1750)$. It shows that the calculated $K\bar{K}$ decay width is consistent with the experimental data ($\Gamma_{K\bar{K}} = 17 \pm 5$ MeV) in Ref. [53]. Similar to the situation of $f_2(1640)$ and $f_2(1565)$ discussed above, the issue of whether $f_2(1810)$ and $f_2(1750)$ can be categorized as the same state should be clarified in future experiment, especially by the measurement of the resonance parameters of $f_2(1810)$ and $f_2(1750)$.

C. $n^{2S+1}L_J = 3^3P_2$ tensor mesons

According to the analysis of mass spectrum in Fig. 1, $f_2(1910)$ and $f_2(1950)$ can be candidates of the second radial excitation of $f_2(1270)$. Since the masses of $f_2(1910)$ and $f_2(1950)$ are close to each other, it is difficult to distinguish them only by the mass analysis. We notice the large difference of the widths of $f_2(1910)$ and $f_2(1950)$. Namely, the average value of the width of $f_2(1950)$ is 472 ± 18 MeV, which is significantly larger than that of $f_2(1910)$, i.e., $\Gamma_{f_2(1910)} = 196 \pm 31$ MeV [1]. Thus, the strong decay study of tensor meson with 3^3P_2 can tell us which state is suitable to be categorized as the candidate of the second radial excitation of $f_2(1270)$.

As shown in Fig. 5, under the 3^3P_2 assignment to $f_2(1910)$, the calculated total width of the $f_2(1910)$ two-body strong decays is in agreement with the experimental width given in Ref. [34], where we take $R = 4.55$–4.70 GeV^{-1}. Our calculation also provides the information of its dominant decay ($\pi\pi$) and other sizeable decays ($\pi\pi(1300)$, $\pi\pi_2(1670)$, $\pi a_1(1260)$, $\rho\rho$, $\omega\omega$, and $K\bar{K}$). The data for $f_2(1910) \to K\bar{K}$, $\eta\eta$, $\omega\omega$, $\eta\eta'$, and $\rho\rho$ are available in experiment [1], and we present several ratios between the partial decay widths to compare with the data:

$$\frac{\Gamma_{\omega\omega}}{\Gamma_{\eta\eta'}} = 1.8\text{–}2.9, \qquad \frac{\Gamma_{\rho\rho}}{\Gamma_{\omega\omega}} = 3.4\text{–}3.8 \tag{7}$$

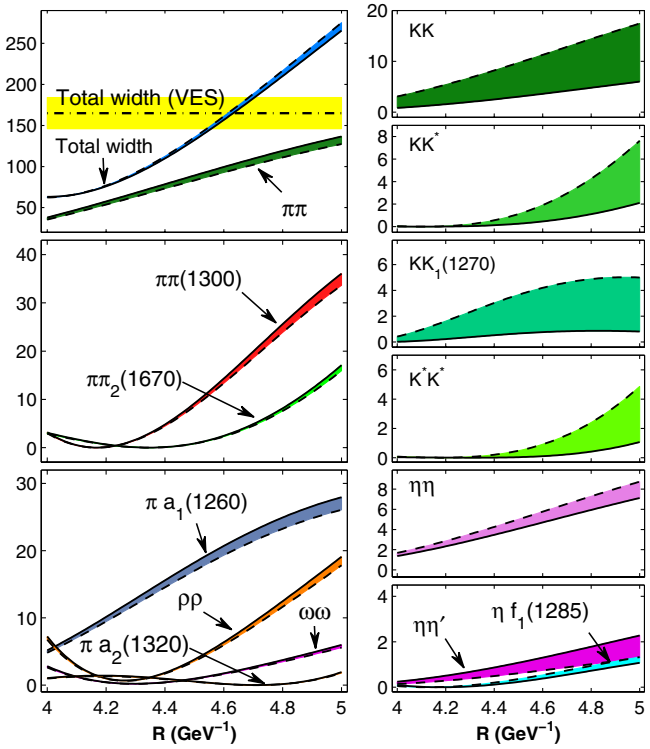

FIG. 5 (color online). The partial decay width of $f_2(1910)$ dependent on the R value and the comparison with the experimental data (the dash-dot lines with yellow band from Ref. [34]). The partial widths presented here are arranged in the same way as in Fig. 3.

with $R = 4.55$–4.70 GeV^{-1}. The corresponding measurements are $\Gamma_{\omega\omega}/\Gamma_{\eta\eta'} = 2.6 \pm 0.6$ and $\Gamma_{\rho\rho}/\Gamma_{\omega\omega} = 2.6 \pm 0.4$ [51], respectively.

Furthermore, it shows that $f_2(1950)$ is not favored to be classified as the second radial excitation of $f_2(1270)$ since the obtained total width in Fig. 5 are far smaller than the width of $f_2(1950)$.

In the following analysis, we discuss the second radial excitation of $f_2'(1525)$. In Table. I, there are 2 states $f_2(2140)$ and $f_2(2150)$ with masses near that obtained by the analysis of Regge trajectories, although $f_2(2140)$ is not a well established state in PDG [1]. In our analysis, we take the mass of the second radial excitation of $f_2'(1525)$ as 2140 MeV, and study its decay behavior to compare with the experimental data of $f_2(2140)$ and $f_2(2150)$.

Sizeable decay modes of the second radial excitation of $f_2'(1525)$ include $K\bar{K}$, $K\bar{K}^* + \text{H.c.}$, $K^*\bar{K}^*$, and $KK_1(1270) + \text{H.c.}$, which suggests the dominance of strange meson pair decays for $f_2'(1525)$. The calculated total width supports $f_2(2150)$ as the candidate of the second radial excitation of $f_2'(1525)$ with $R = 4.16$–4.51 GeV^{-1}. It overlaps with the average width of $f_2(2150)$ ($\Gamma_{f_2(2150)} = 152 \pm 30$ MeV) but deviates from that of $f_2(2140)$ ($\Gamma_{f_2(2140)} = 49 \pm 28$ MeV) [1]. The results presented in Fig. 6 provide a guidance for further

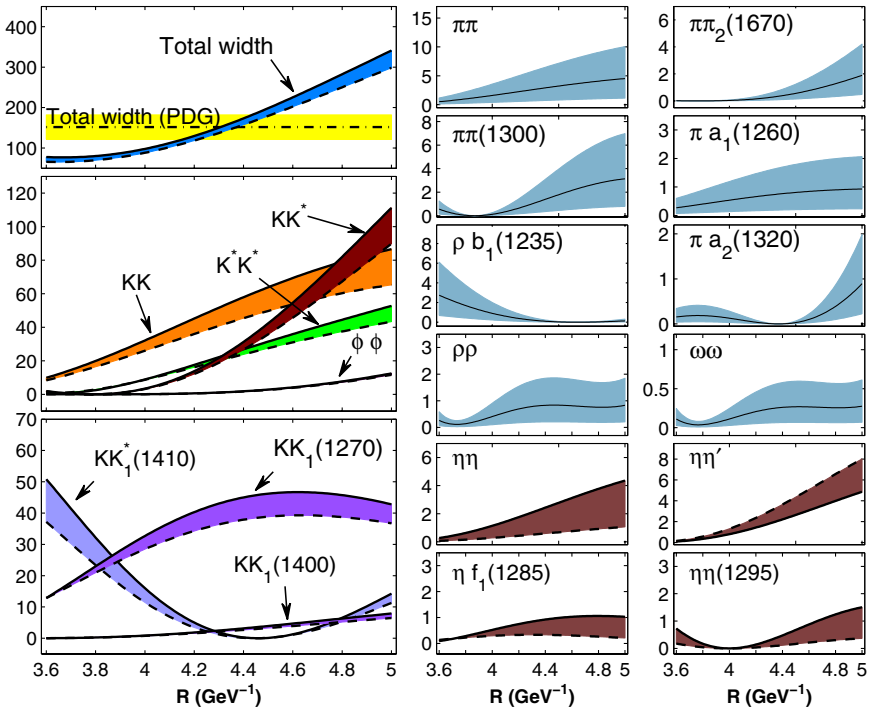

FIG. 6 (color online). The two-body strong decay behavior of the second radial excitation of $f_2'(1525)$ dependent on the R value and mixing angle ϕ. The solid and dashed lines in each diagram correspond to the results taking the typical value $\phi = 85°$ and $\phi = 75°$, respectively. Here, the experimental width (the dash-dot line with yellow band) of $f_2(2150)$ is taken from Ref. [1]. The bands appearing in the diagrams corresponding to $\rho b_1(1235)$, $\pi\pi_2(1670)$, $\pi\pi$, $\pi a_2(1320)$, $\pi\pi(1300)$, $\pi a_1(1260)$, $\rho\rho$, $\omega\omega$ channels are due to $\phi = (75\text{–}85)°$ taken in our calculation, where the solid lines are the typical values with $\phi = 80°$.

experimental study of the second radial excitation of $f_2'(1525)$.

D. $n^{2S+1}L_J = 4^3P_2$ tensor mesons

According to the analysis of mass spectrum shown in Fig. 1, the masses of the third radial excitations of $f_2(1270)$ and $f_2'(1525)$ are around 2219 and 2372 MeV, respectively. It thus makes $f_2(2240)$ and $f_2(2410)$ good candidates for the third radial excitations. The calculations of their partial decay widths and total widths of two-body strong decays are presented in Figs. 7 and 8.

From Fig. 7, it shows that the decay of $f_2(2240)$ is dominated by the $\pi\pi$ and $\pi\pi(1300)$ channels. Other sizeable decay channels include $\rho\rho$, $\pi\pi_2(1670)$, $\pi a_1(1260)$, $\eta\eta$, and $\eta\eta'$ etc. As the candidate of the third radial excitation of $f_2'(1525)$, $f_2(2410)$ mainly decays into strange meson pairs due to the dominance of the $s\bar{s}$ component in its wave function. As shown in Fig. 8, the $f_2(2410) \to K\bar{K}$ is dominant while other decay channels such as $K\bar{K}^* + \text{H.c.}$, $K\bar{K}_1(1270) + \text{H.c.}$, $K\bar{K}_1(1400)$, and $K^*\bar{K}^*$ are also important.

Although $f_2(2240)$ and $f_2(2410)$ can be taken as good candidates for the third radial excitations of $f_2(1270)$ and $f_2'(1525)$, respectively, detailed experimental information is still absent for further understanding of their properties. It should be useful to compare the calculated decay widths shown in Figs. 7 and 8 with future experimental measurements in order to gain further insights into the nature of these two states.

E. $n^{2S+1}L_J = 1^3F_2$ tensor mesons

In Fig. 9, we present the partial decay widths of the ground state F-wave tensor meson with 1^3F_2. Assuming that it is dominated by the $n\bar{n}$ component, we use the mass of $f_2(2010)$ as the input to calculate the partial decays widths. It shows that the width of the 1^3F_2 tensor meson is very broad. Some of those dominant decay channels can be seen in Fig. 9 in terms of R, e.g., $f_2(2010) \to \pi\pi_2(1670)$ and $\pi a_2(1260)$.

In this work, we also study the two-body decays of the 2^3F_2 tensor meson, which is the second radial excitation of 1^3F_2. With the mass of $f_2(2300)$ as the input, the calculated partial decay widths are shown in Fig. 10. A sum of these two-body decay partial widths also gives a broad total width for this state.

At present, the experimental information for $f_2(2010)$, $f_2(2300)$ and $f_2(2340)$ is not enough to help us establish them as the candidates of 1^3F_2 and 2^3F_2 tensor mesons. We also expect more experimental measurements in the future would be able to clarify their properties.

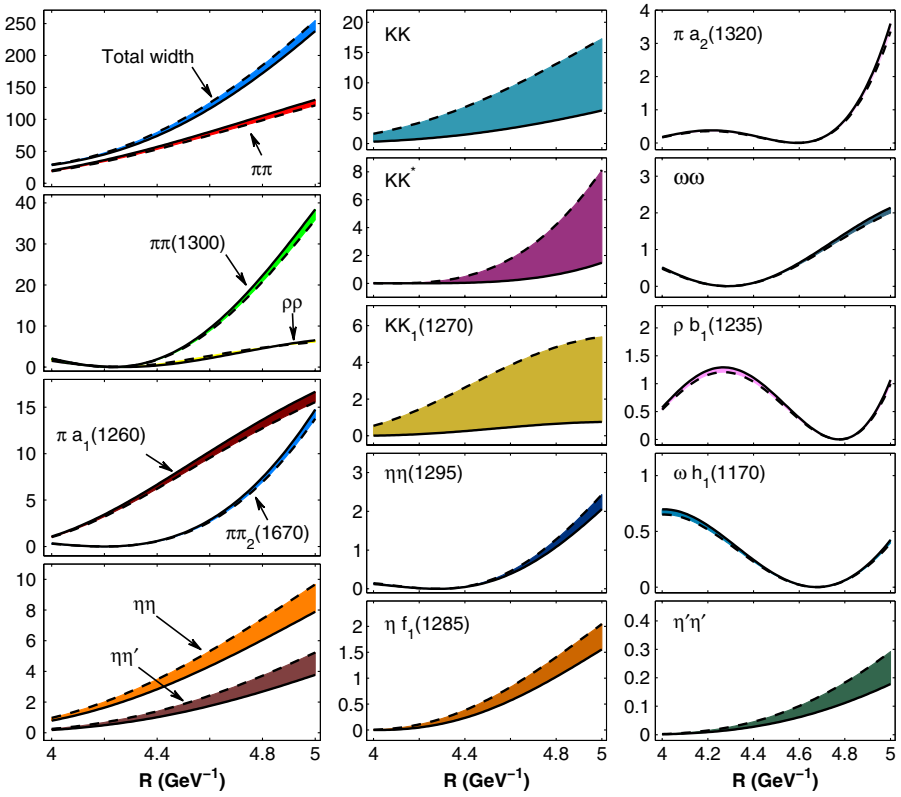

FIG. 7 (color online). The partial decay width of the third radial excitation of $f_2(1270)$ dependent on the R value. The partial widths presented here are arranged in the same way as in Fig. 3.

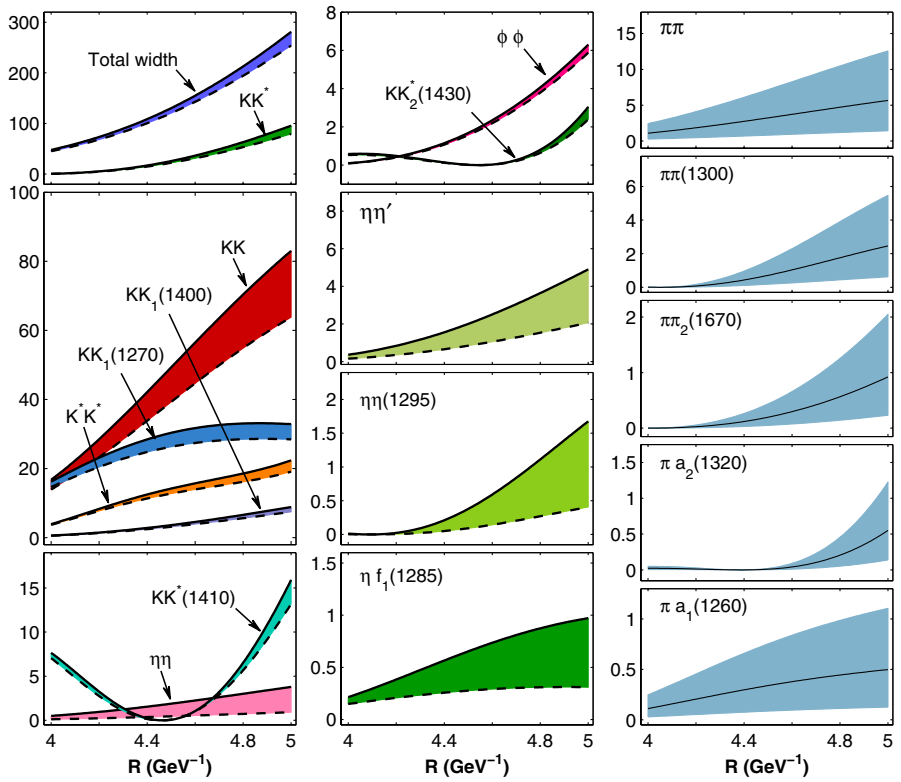

FIG. 8 (color online). The two-body strong decay behavior of the third radial excitation of $f_2'(1525)$ dependent on the R value and mixing angle ϕ. The partial widths presented here are arranged in the same way as in Fig. 4.

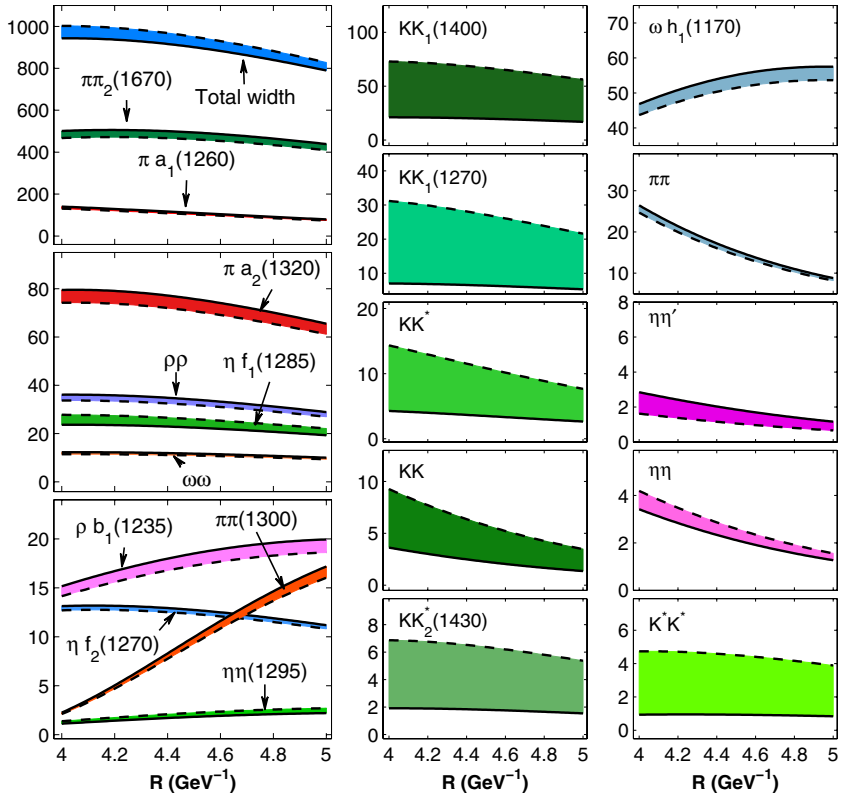

FIG. 9 (color online). The partial decay width of tensor meson with 1^3F_2 quantum number dependent on the R value. The partial widths presented here are arranged in the same way as in Fig. 3.

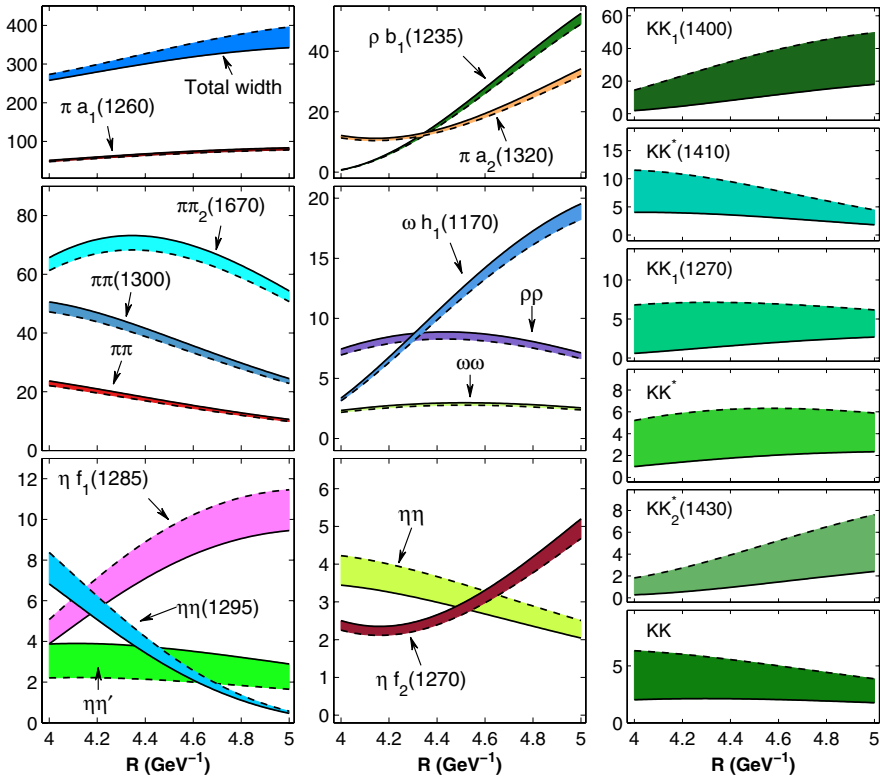

FIG. 10 (color online). The partial decay width of tensor meson with 2^3F_2 quantum number dependent on the R value. The partial widths presented here are arranged in the same way as in Fig. 3.

V. DISCUSSION AND CONCLUSION

So far there have been a large number of isoscalar tensor states observed in experiment [1]. A crucial task is to understand their properties and try to categorize them into the hadron spectrum. In this work we carry out a systematic study of these isoscalar tensor states by performing an analysis of the mass spectrum and calculating their two-body strong decays in the QCP model. By comparing our results with the available experimental data, we extract important information for a better understanding of the underlying structures of these f_2 states.

By the analysis of mass spectrum based on the Regge trajectories of tensor states, we identify candidates for the radial excitations of the P-wave and F-wave states. By calculating the partial decay widths of those states into various two-body final state hadrons and comparing the results with the available experimental information, we succeed in categorizing some of those states into the $q\bar{q}$ radial excitation spectrum. Meanwhile, some obvious controversies are also exposed, for which further theoretical and experimental studies are needed. In particular, at present, only $f_2(1270)/f_2'(1525)$ have a relatively well-established experimental status, while experimental information for other observed higher f_2 states is still limited. Although $f_J(2220)$ has been proposed to be a tensor glueball candidate in the literature [64,73], further study of the tensor glueball is still needed in order to single it out from experimental observables. Improved experimental measurements of those higher f_2 states would be crucial for distinguish the conventional $q\bar{q}$ scenario from other possible exotic configurations.

ACKNOWLEDGMENTS

This project is supported in part by the National Natural Science Foundation of China (Grants No. 11175073 and No. 11035006), the Ministry of Education of China (FANEDD under Grant No. 200924, DPFIHE under Grant No. 20090211120029, NCET under Grant No. NCET-10-0442, and the Fundamental Research Funds for the Central Universities), the Fok Ying-Tong Education Foundation (No. 131006), and the Chinese Academy of Sciences (KJCX2-EW-N01).

[1] K. Nakamura *et al.* (Particle Data Group), J. Phys. G **37**, 075021 (2010).
[2] K. Boesebeck and M. Deutschmann, Nucl. Phys. **B4**, 501 (1968).
[3] W. D. Apel *et al.* (Serpukhov-CERN Collaboration), Phys. Lett. **57B**, 398 (1975).
[4] W. D. Apel, K. H. Augenstein, E. Bertolucci, S. V. Donskov, A. V. Inyakin, V. A. Kachanov, R. N. Krasnokutsky, M. Kruger *et al.*, Nucl. Phys. **B201**, 197 (1982).
[5] D. Alde *et al.* (GAMS Collaboration), Eur. Phys. J. A **3**, 361 (1998).
[6] R. S. Longacre, A. Etkin, K. J. Foley, W. A. Love, T. W. Morris, A. C. Saulys, E. D. Platner, S. J. Lindenbaum *et al.*, Phys. Lett. B **177**, 223 (1986).
[7] D. Alde *et al.* (Serpukhov-Brussels-Los Alamos-Annecy (LAPP) Collaboration), Phys. Lett. B **198**, 286 (1987).
[8] M. Ablikim *et al.* (BES Collaboration), Phys. Lett. B **607**, 243 (2005).
[9] M. Ablikim, J. Z. Bai, Y. Ban, J. G. Bian, X. Cai, H. F. Chen, H. S. Chen, H. X. Chen *et al.*, Phys. Lett. B **642**, 441 (2006).
[10] D. J. Crennell, G. R. Kalbfleisch, K. W. Lai, M. Scarr, T. G. Schumann, I. O. Skillicorn, and M. S. Webster, Phys. Rev. Lett. **16**, 1025 (1966).
[11] L. Gorlich *et al.* (CERN-Cracow-Munich Collaboration), Nucl. Phys. **B174**, 16 (1980).
[12] V. Chabaud *et al.* (CERN-CRACOW-MUNICH Collaboration), Acta Phys. Pol. B **12**, 575 (1981).
[13] J. Becker *et al.* (Mark-III Collaboration), Phys. Rev. D **35**, 2077 (1987).
[14] J. E. Augustin *et al.* (DM2 Collaboration), Phys. Rev. Lett. **60**, 2238 (1988).
[15] J. Z. Bai *et al.* (BES Collaboration), Phys. Rev. Lett. **77**, 3959 (1996).
[16] J. Z. Bai *et al.* (BES Collaboration), Phys. Rev. D **68**, 052003 (2003).
[17] M. Doser *et al.* (ASTERIX Collaboration), Phys. Lett. B **215**, 792 (1988); Nucl. Phys. B, Proc. Suppl. **8**, 213 (1989).
[18] F. Antinori *et al.* (WA91 Collaboration), Phys. Lett. B **353**, 589 (1995).
[19] D. Barberis *et al.* (102 Collaboration), Phys. Lett. B **413**, 217 (1997).
[20] D. Barberis *et al.* (WA102 Collaboration), Phys. Lett. B **471**, 440 (2000).
[21] J. Z. Bai *et al.* (BES Collaboration), Phys. Lett. B **472**, 207 (2000).
[22] A. Etkin, K. J. Foley, R. S. Longacre, W. A. Love, T. W. Morris, E. D. Platner, V. A. Polychronakos, A. C. Saulys *et al.*, Phys. Rev. Lett. **49**, 1620 (1982).
[23] A. Etkin, K. J. Foley, R. S. Longacre, W. A. Love, T. W. Morris, E. D. Platner, A. C. Saulys, S. J. Lindenbaum, C. S. Chan, and M. A. Kramer, Phys. Lett. **165B**, 217 (1985).
[24] A. Etkin, K. J. Foley, R. W. Hackenburg, R. S. Longacre, W. A. Love, T. W. Morris, E. D. Platner, A. C. Saulys *et al.*, Phys. Lett. B **201**, 568 (1988).
[25] B. V. Bolonkin, S. K. Bloshenko, V. V. Vladimirsky, Y. P. Gorin, V. K. Grigorev, A. P. Grishin, I. A. Erofeev, O. N. Erofeeva *et al.*, Yad. Fiz. **46**, 799 (1987).
[26] V. V. Vladimirsky, V. K. Grigorev, I. A. Erofeev, O. N. Erofeeva, Y. V. Katinov, V. I. Lisin, V. N. Luzin, V. N. Nozdrachev *et al.*, Phys. At. Nucl. **69**, 493 (2006).

[27] P. S. L. Booth, L. J. Carroll, R. A. Donald, D. N. Edwards, D. Frame, B. R. French, M. A. Houlden, I. S. Hughes *et al.*, Nucl. Phys. **B273**, 677 (1986).

[28] K. Abe *et al.* (Belle Collaboration), Eur. Phys. J. C **32**, 323 (2003).

[29] I. Uman, D. Joffe, Z. Metreveli, K. K. Seth, A. Tomaradze, and P. K. Zweber, Phys. Rev. D **73**, 052009 (2006).

[30] W. Beusch, W. E. Fischer, B. Gobbi, P. Astbury, Phys. Lett. **25B**, 357 (1967).

[31] C. Daum *et al.* (ACCMOR Collaboration), Z. Phys. C **23**, 339 (1984).

[32] V. V. Vladimirsky, V. K. Grigorev, O. N. Erofeeva, Y. V. Katinov, V. I. Lisin, V. N. Luzin, V. N. Nozdrachev, V. V. Sokolovsky, G. D. Tikhomirov and Y. P. Shkurenko, Phys. At. Nucl. **64**, 1895 (2001).

[33] T. Akesson *et al.* (Axial Field Spectrometer Collaboration), Nucl. Phys. **B264**, 154 (1986).

[34] D. V. Amelin, D. V. Bugg, Y. G. Gavrilov, Y. P. Gouz, R. I. Dzhelyadin, V. A. Dorofeev, A. M. Zaitsev, A. V. Zenin *et al.*, Phys. At. Nucl. **69**, 690 (2006).

[35] D. V. Amelin *et al.* (VES Collaboration), Nucl. Phys. **A668**, 83 (2000).

[36] C. Amsler *et al.* (Crystal Barrel Collaboration), Eur. Phys. J. C **23**, 29 (2002).

[37] A. Bertin *et al.* (OBELIX Collaboration), Phys. Lett. B **408**, 476 (1997).

[38] B. May *et al.* (ASTERIX Collaboration), Z. Phys. C **46**, 203 (1990).

[39] A. Bertin *et al.* (OBELIX Collaboration), Phys. Rev. D **57**, 55 (1998).

[40] D. Alde *et al.* (IHEP-IISN-LANL-LAPP-TSUIHEP Collaboration), Phys. Lett. B **216**, 451 (1989).

[41] A. Adamo, M. Agnello, F. Balestra, G. Belli, G. Bendiscioli, A. Bertin, P. Boccaccio, G. C. Bonazzola *et al.*, Phys. Lett. B **287**, 368 (1992).

[42] D. V. Bugg, I. Scott, B. S. Zou, V. V. Anisovich, A. V. Sarantsev, T. H. Burnett, and S. Sutlief, Phys. Lett. B **353**, 378 (1995).

[43] C. Amsler *et al.* (Crystal Barrel Collaboration), Phys. Lett. B **639**, 165 (2006).

[44] G. Costa *et al.* (BARI-BONN-CERN-GLASGOW-LIVERPOOL-MILAN-VIENNA Collaboration), Nucl. Phys. **B175**, 402 (1980).

[45] N. M. Cason, N. N. Biswas, A. E. Baumbaugh, J. M. Bishop, P. E. Cannata, L. J. Dauwe, V. P. Kenney, R. C. Ruchti, W. D. Shephard, and J. M. Watson, Phys. Rev. Lett. **48**, 1316 (1982).

[46] D. Alde *et al.* (Serpukhov-Brussels-Los Alamos-Annecy (LAPP) Collaboration), Nucl. Phys. **B269**, 485 (1986).

[47] D. Alde *et al.* (IHEP-IISN-LANL-LAPP-PISA Collaboration), Sov. J. Nucl. Phys. **47**, 810 (1988).

[48] S. Uehara *et al.* (Belle Collaboration), Phys. Rev. D **82**, 114031 (2010).

[49] A. V. Anisovich, D. V. Bugg, V. A. Nikonov, A. V. Sarantsev, and V. V. Sarantsev, Phys. Rev. D **85**, 014001 (2012).

[50] D. Alde *et al.* (IHEP-IISN-LANL-LAPP-TSUIHEP Collaboration), Phys. Lett. B **241**, 600 (1990).

[51] D. Barberis *et al.* (WA102 Collaboration), Phys. Lett. B **484**, 198 (2000).

[52] D. Barberis *et al.* (WA102 Collaboration), Phys. Lett. B **479**, 59 (2000).

[53] V. A. Shchegelsky, A. V. Sarantsev, V. A. Nikonov, A. V. Anisovich, Eur. Phys. J. A **27**, 207 (2006).

[54] D. R. Green, H. C. Fenker, K. W. Lai, J. LeBritton, Y. C. Lin, A. E. Pifer, T. F. Davenport, J. H. Goldman *et al.*, Phys. Rev. Lett. **56**, 1639 (1986).

[55] H. Chen, J. Sexton, A. Vaccarino, and D. Weingarten, Nucl. Phys. B, Proc. Suppl. **34**, 357 (1994).

[56] C. J. Morningstar and M. J. Peardon, Phys. Rev. D **60**, 034509 (1999).

[57] D. V. Bugg and B. S. Zou, Phys. Lett. B **396**, 295 (1997).

[58] T. Barnes, F. E. Close, P. R. Page, and E. S. Swanson, Phys. Rev. D **55**, 4157 (1997).

[59] T. Barnes, N. Black, and P. R. Page, Phys. Rev. D **68**, 054014 (2003).

[60] L. S. Celenza, B. Huang, H. Wang, and C. M. Shakin, Phys. Rev. C **60**, 035206 (1999).

[61] A. Dobado and J. R. Pelaez, Phys. Rev. D **65**, 077502 (2002).

[62] D. Ebert, R. N. Faustov, and V. O. Galkin, Phys. Rev. D **79**, 114029 (2009).

[63] Y. S. Surovtsev, P. Bydzovsky, R. Kaminski, and M. Nagy, arXiv:1104.0538.

[64] F. Giacosa, T. Gutsche, V. E. Lyubovitskij, and A. Faessler, Phys. Rev. D **72**, 114021 (2005).

[65] D.-M. Li, H. Yu, and Q.-X. Shen, J. Phys. G **27**, 807 (2001).

[66] H.-Y. Cheng and R. Shrock, Phys. Rev. D **84**, 094008 (2011).

[67] L. Roca and E. Oset, Phys. Rev. D **82**, 054013 (2010).

[68] A. M. Torres, L. S. Geng, L. R. Dai, B. X. Sun, E. Oset, and B. S. Zou, Phys. Lett. B **680**, 310 (2009).

[69] L. S. Geng, E. Oset, R. Molina, A. M. Torres, T. Branz, F. K. Guo, L. R. Dai, and B. X. Sun, AIP Conf. Proc. **1322**, 214 (2010).

[70] L. S. Geng, F. K. Guo, C. Hanhart, R. Molina, E. Oset, and B. S. Zou, Eur. Phys. J. A **44**, 305 (2010).

[71] T. Branz, L. S. Geng, and E. Oset, Phys. Rev. D **81**, 054037 (2010).

[72] J. P. Ma, Nucl. Phys. **B605**, 625 (2001); **B611**, 523(E) (2001).

[73] L. Burakovsky and P. R. Page, Phys. Rev. D **62**, 014011 (2000).

[74] F. Buisseret, Phys. Rev. C **76**, 025206 (2007).

[75] B. A. Li, Phys. Rev. D **86**, 017501 (2012).

[76] V. V. Anisovich, Phys. Usp. **38**, 1179 (1995) [Usp. Fiz. Nauk **165**, 1225 (1995)].

[77] V. V. Anisovich, M. A. Matveev, J. Nyiri, and A. V. Sarantsev, Int. J. Mod. Phys. A **20**, 6327 (2005).

[78] V. Crede and C. A. Meyer, Prog. Part. Nucl. Phys. **63**, 74 (2009).

[79] E. Klempt and A. Zaitsev, Phys. Rep. **454**, 1 (2007).

[80] A. V. Anisovich, V. V. Anisovich, and A. V. Sarantsev, Phys. Rev. D **62**, 051502 (2000).

[81] L. Micu, Nucl. Phys. **B10**, 521 (1969).

[82] A. L. Yaouanc, L. Oliver, O. Pène, and J. Raynal, Phys. Rev. D **8**, 2223 (1973); **9**, 1415 (1974); **11**, 1272 (1975); Phys. Lett. **72**, 57 (1977); **71B**, 397 (1977).

[83] A. L. Yaouanc, L. Oliver, O. Pene, and J. C. Raynal, Phys. Lett. **72B**, 57 (1977).

[84] A. L. Yaouanc, L. Oliver, O. Pene, and J. C. Raynal, *Hadron Transitions of the Quark Model* (Gordon and Breach, New York, 1988).

[85] E. van Beveren, C. Dullemond, and G. Rupp, Phys. Rev. D **21**, 772 (1980); **22**, 787(E) (1980).
[86] E. van Beveren, G. Rupp, T. A. Rijken, and C. Dullemond, Phys. Rev. D **27**, 1527 (1983).
[87] R. Bonnaz, B. Silvestre-Brac, and C. Gignoux, Eur. Phys. J. A **13**, 363 (2002).
[88] W. Roberts and B. Silvestre-Brac, Few-Body Syst. **11**, 171 (1992).
[89] J. Lu, W. Z. Deng, X. L. Chen, and S. L. Zhu, Phys. Rev. D **73**, 054012 (2006).
[90] Z. G. Luo, X. L. Chen, and X. Liu, Phys. Rev. D **79**, 074020 (2009).
[91] H. G. Blundell and S. Godfrey, Phys. Rev. D **53**, 3700 (1996).
[92] P. R. Page, Nucl. Phys. **B446**, 189 (1995).
[93] S. Capstick and N. Isgur, Phys. Rev. D **34**, 2809 (1986).
[94] S. Capstick and W. Roberts, Phys. Rev. D **49**, 4570 (1994).
[95] E. S. Ackleh, T. Barnes, and E. S. Swanson, Phys. Rev. D **54**, 6811 (1996).
[96] F. E. Close and E. S. Swanson, Phys. Rev. D **72**, 094004 (2005).
[97] H. Q. Zhou, R. G. Ping, and B. S. Zou, Phys. Lett. B **611**, 123 (2005).
[98] X. H. Guo, H. W. Ke, X. Q. Li, X. Liu, and S. M. Zhao, Commun. Theor. Phys. **48**, 509 (2007).
[99] B. Zhang, X. Liu, W.-Z. Deng, and S.-L. Zhu, Eur. Phys. J. C **50**, 617 (2007).
[100] C. Chen, X. L. Chen, X. Liu, W. Z. Deng, and S. L. Zhu, Phys. Rev. D **75**, 094017 (2007); X. Liu, C. Chen, W. Z. Deng, and X. L. Chen, Chinese Phys. C **32**, 424 (2008).
[101] D. M. Li and B. Ma, Phys. Rev. D **77**, 074004 (2008); D. M. Li and B. Ma, Phys. Rev. D **77**, 094021 (2008); D. M. Li and S. Zhou, Phys. Rev. D **78**, 054013 (2008); **79**, 014014 (2009).
[102] Z.-F. Sun and X. Liu, Phys. Rev. D **80**, 074037 (2009).
[103] X. Liu, Z.-G. Luo, and Z.-F. Sun, Phys. Rev. Lett. **104**, 122001 (2010).
[104] Z.-F. Sun, J.-S. Yu, X. Liu, and T. Matsuki, Phys. Rev. D **82**, 111501 (2010).
[105] J.-S. Yu, Z.-F. Sun, X. Liu, and Q. Zhao, Phys. Rev. D **83**, 114007 (2011).
[106] X. Wang, Z.-F. Sun, D.-Y. Chen, X. Liu, and T. Matsuki, Phys. Rev. D **85**, 074024 (2012).
[107] M. Jacob and G. C. Wick, Ann. Phys. (N.Y.) **7**, 404 (1959); **281**, 774 (2000).
[108] G. D. Tikhomirov, I. A. Erofeev, O. N. Erofeeva, and V. N. Luzin, Phys. At. Nucl. **66**, 828 (2003) Yad. Fiz. **66**, 860 (2003).
[109] M. Acciarri *et al.* (L3 Collaboration), Phys. Lett. B **501**, 173 (2001).
[110] D. Aston, N. Awaji, T. Bienz, F. Bird, J. D'Amore, W. M. Dunwoodie, R. Endorf, K. Fujii *et al.*, Nucl. Phys. **B301**, 525 (1988).
[111] A. Falvard *et al.* (DM2 Collaboration), Phys. Rev. D **38**, 2706 (1988).
[112] J. E. Augustin *et al.* (DM2 Collaboration), Z. Phys. C **36**, 369 (1987).
[113] C. A. Baker, B. M. Barnett, C. J. Batty, K. Braune, D. V. Bugg, O. Cramer, V. Crede, and N. Djaoshvili *et al.*, Phys. Lett. B **467**, 147 (1999).